



|            |  |
|------------|--|
| Title      | Genetic diversity, paraphyly and incomplete lineage sorting of mtDNA, ITS2 and microsatellite flanking region in closely related <i>Heliopora</i> species (Octocorallia) |
| Author(s)  | Yasuda, Nina; Taquet, Coralie; Nagai, Satoshi; Fortes, Miguel; Fan, Tung-Yung; Harii, Saki; Yoshida, Terutoyo; Sito, Yuta; Nadaoka, Kazuo                                |
| Citation   | Molecular Phylogenetics and Evolution, 93: 161-171   |
| Issue Date | 2015-12  |
| URL        | <a href="http://hdl.handle.net/20.500.12000/47246">http://hdl.handle.net/20.500.12000/47246</a>  |
| Rights     | Creative Commons Attribution-NonCommercial-NoDerivatives 4.0   |



Contents lists available at ScienceDirect

## Molecular Phylogenetics and Evolution

journal homepage: [www.elsevier.com/locate/ympev](http://www.elsevier.com/locate/ympev)

# Genetic diversity, paraphyly and incomplete lineage sorting of mtDNA, ITS2 and microsatellite flanking region in closely related *Heliopora* species (Octocorallia) <sup>☆</sup>



Nina Yasuda <sup>a,\*</sup>, Coralie Taquet <sup>b</sup>, Satoshi Nagai <sup>c</sup>, Miguel Fortes <sup>d</sup>, Tung-Yung Fan <sup>e</sup>, Saki Harii <sup>f</sup>, Terutoyo Yoshida <sup>g</sup>, Yuta Sito <sup>g</sup>, Kazuo Nadaoka <sup>h</sup>

<sup>a</sup> Organization for Promotion of Tenure Track, University of Miyazaki, Gakuen-kibanadai-nishi-1-1, Miyazaki 889-2192, Japan

<sup>b</sup> UMR 241 Ecosystèmes Insulaires Océaniques, Université de la Polynésie Française, B.P. 6570, 98702 FAA'A Aéroport, Tahiti, French Polynesia

<sup>c</sup> National Research Institute of Fisheries Science, Aquatic Genomics Research Center, 2-12-4 Fukuura, Kanazawa-k, Yokohama, Kanagawa 236-8648, Japan

<sup>d</sup> Marine Science Institute CS, University of the Philippines, Diliman, Quezon City 1101, Philippines

<sup>e</sup> National Museum of Marine Biology and Aquarium, 2 Houwan Road, Checheng, Pingtung, Taiwan, ROC

<sup>f</sup> Tropical Biosphere Research Center, University of the Ryukyus, 3422 Sesoko, Motobu, Okinawa 905-0227, Japan

<sup>g</sup> Department of Marine Biology and Environmental Sciences, Faculty of Agriculture, University of Miyazaki, Gakuen-kibanadai-nishi-1-1, Miyazaki 889-2192, Japan

<sup>h</sup> Graduate School of Information Science and Engineering, Tokyo Institute of Technology, O-okayama 2-12-1, Meguro-ku, Tokyo 152-8552, Japan

## ARTICLE INFO

## Article history:

Received 10 June 2014

Revised 14 July 2015

Accepted 15 July 2015

Available online 29 July 2015

## Keywords:

ITS2

Concerted evolution

*mtMutS*

Secondary structure

Species identification

Speciation

## ABSTRACT

Examining genetic diversity and lineage sorting of different genes in closely related species provide useful information for phylogenetic analyses and ultimately for understanding the origins of biodiversity. In this study, we examined inter- and intraspecific genetic variation in internal transcribed spacer 2 (ITS2), partial mitochondrial gene (*mtMutS*), and nuclear microsatellite flanking region in two closely related octocoral species (*Heliopora coerulea*, HC-A and HC-B). These species were recently identified in a population genetic study using microsatellite markers. The two species have different reproductive timing, which ecologically promotes lineage sorting. In this study, we examined whether species boundaries could be detected by the commonly used nuclear ITS2 and *mtMutS*, as well as by possibly neutral microsatellite flanking sequences. Haplotype network analysis of microsatellite flanking region revealed that a possible ancestral haplotype was still shared between the two species, indicating on-going lineage sorting. Haplotype network analysis of ITS2 and microsatellite flanking region revealed shared haplotypes between the two lineages. The two species shared fewer ITS2 sequences than microsatellite flanking region sequences. The almost fixed point mutation at the tip of helix 3 of ITS2 was not associated with the secondary structure or compensatory base changes (CBCs). The phylogenetic tree of ITS2 showed paraphyly and that of the microsatellite flanking region indicated that lineage sorting for the two species may be incomplete. Much higher intra- and inter-individual variation of ITS2 was observed in HC-B than that in HC-A, highlighting the importance of examining ITS2 from multiple individuals to estimate genetic diversity. The mitochondrial *mtMutS* gene sequences from 39 individuals, including both species collected from Japan and Taiwan, showed no variation because of slow rates of mitochondrial nucleotide substitution. This study suggests caution is warranted when reciprocal monophyly in a phylogenetic tree is used as the criterion for delimiting closely related octocoral species based on ITS2 or *mtMutS* sequences. Detection of boundaries between closely related species requires multi-locus analysis, such as genetic admixture analysis using multiple individuals.

© 2015 The Authors. Published by Elsevier Inc. This is an open access article under the CC BY-NC-ND license (<http://creativecommons.org/licenses/by-nc-nd/4.0/>).

## 1. Introduction

Examining genetic diversity and lineage sorting of different genes in closely related species provides significant information for species delimitation and phylogenetic analysis. Ultimately, such examination provides insights for understanding the origin of biodiversity. Species delimitation is important for assessing

<sup>☆</sup> This paper was edited by the Associate Editor Bernd Schierwater.

\* Corresponding author at: University of Miyazaki, Faculty of Agriculture, Department of Marine Biology and Environmental Sciences, Gakuen-kibanadai-nishi-1-1, Miyazaki 889-2192, Japan. Fax: +81 985 58 2884.

E-mail address: [ninayausda@gmail.com](mailto:ninayausda@gmail.com) (N. Yasuda).

biodiversity and conserving natural resources. Misunderstanding of species boundaries can result in over or under estimation of geographic distribution, population abundance, and population risks (Kim et al., 2004; Prada et al., 2008). As genetic methods became more economical and accessible, phylogenetic analysis made it possible to reveal hidden species diversity that was undetectable using morphological analysis. Genetic identification techniques, such as DNA barcoding (Hebert et al., 2003) and reciprocal monophyly in phylogenetic trees, are increasingly popular tools for species determination. There are a number of advantages to using genetic methods of species delimitation when morphological identification is difficult, including simplicity and objectivity. The accuracy of genetic identification depends on the availability of fixed species-specific variations. Mitochondrial DNA, especially the partial cytochrome c oxidase subunit 1 (COI) mitochondrial region, is often used for DNA barcoding of higher animal species (Hebert et al., 2003; Waugh, 2007). Other genetic markers such as plant-specific matK, rbcL, and psbA can be used for DNA barcoding of plant species (Hollingsworth et al., 2011; Yang et al., 2012). Second internal transcribed spacer (ITS2) and other mitochondrial genes (e.g., *mtMutS*) are used for basal animal species DNA barcoding (Dolan et al., 2013; McFadden et al., 2006; Mi-Hyun et al., 2007; Wörheide, 2006). However, there are challenges to species identification using genetic markers in closely related species (Moritz and Cicero, 2004). These challenges include incomplete lineage sorting (Funk and Omland, 2003), introgression (Chase et al., 2005), the presence of pseudogenes (Lorenz et al., 2005), intra-individual diversity in some multiple-copy families of genes (Dover, 1982), and low substitution rates of mitochondrial genes in some taxa, such as plants (Shearer et al., 2002; Waugh, 2007), sponges (Mi-Hyun et al., 2007; Wörheide, 2006), and anthozoans (Huang et al., 2008; Shearer et al., 2002).

As gene flow between incipient species becomes restricted, genetic drift causes loss of common ancestral alleles in neutral loci (Kingman, 1982). In multiple-copy gene families, concerted patterns of fixation (concerted evolution) further allow species discontinuities to establish in a manner not predicted by natural selection or genetic drift (Dover, 1982). However, if the time since speciation is too short, the common ancestral alleles remain in both species in the same loci, and incomplete lineage sorting will be observed. Similarly, hybridization between closely related species also hinders reciprocal monophyly. Because sorting of genes of different species always initiates from within-species genetic diversity, examination of both intra- and interspecific genetic variation in closely related species provides important information about molecular evolution that will be useful for species identification and for testing future phylogenetic analyses.

The anthozoan subclass Octocorallia is an invertebrate taxon for which morphological species delimitation is very challenging because of a low number of homologous characteristics, high plasticity, and intra- and interspecific variation. Thus, there is a practical need for genetic differentiation within this taxon (Bayer, 1961; Fabricius et al., 2001). Among several genetic markers, those used most often for Octocorallia are the *mtMutS* gene (Dolan et al., 2013; McFadden et al., 2010), which is the apparent homolog of a DNA mismatch repair gene and considered to evolve faster than other mitochondrial genes (France and Hoover, 2002), and the second internal ITS2, a multiple-copy gene family found within nuclear ribosomal RNA (rRNA) tandem arrays. Although the mitochondrial protein-coding gene *mtMutS* is useful for resolving many octocoral species (Dolan et al., 2013; McFadden et al., 2010), scleractinians generally have very slow rates of mitochondrial DNA evolution (Hellberg, 2006) and attempts to delimit species boundaries have sometimes had limited success (Dolan et al., 2013; France and Hoover, 2002; McFadden et al., 2011; McFadden et al., 2010).

ITS2 has also been used to determine species boundaries and unique secondary structures of ITS2 with substantial sequence variations have been reported for Octocorallia species. ITS2 sequence alignment based on conserved secondary structure has been used for phylogenetic analysis of octocoral species (Sánchez and Dorado, 2008; Aguilar and Sánchez, 2007a,b; Dorado and Sánchez, 2009). However, ITS2 may be invariant between some species and intraindividual variation sometimes obscures phylogenetic relationships (McFadden et al., 2010). Some octocorals have relatively low intraindividual ITS2 diversity (Aguilar and Sánchez, 2007a; Grajales et al., 2007), which enables the use of direct sequencing methods. However, other species (e.g., temperate gorgonians (Calderón et al., 2006), Caribbean Sea octocorals (Torres-Suarez, 2014)), have relatively high levels of ITS2 variability, which hinders direct sequencing. Torres-Suarez (2014) used denaturing gradient gel electrophoresis (DGGE) to detect intraindividual ITS2 variation and found that the presence of compensatory base changes (CBCs) and hemi-CBCs is useful as a complementary tool for detecting species and population boundaries. Although imperfect, *mtMutS* and ITS2 are the most variable regions available for analysis and are commonly used as important genetic markers for phylogenetic analysis (Aguilar and Sánchez, 2007a; Herrera et al., 2010; McFadden et al., 2010). Therefore, additional insights into intra- and interspecific variation in ITS2 and *mtMutS* among closely related octocoral species would be useful for understanding the robustness of these markers for delimitation of octocoral species. In addition to sequencing ITS2 and mtDNA in octocoral species, we sequenced a possibly neutral microsatellite flanking region for comparison. *Heliopora coerulea* is a shallow-water species found in warm tropical Indo-Pacific Oceans. Along with other corals, *H. coerulea* was recently listed as threatened by the International Union for Conservation of Nature and Natural Resources because of habitat degradation. Although *H. coerulea* was considered to be the sole surviving species of the *Helioporidae* (the only Helioporacea family) (Colgan, 1984), our recent population genetic analysis using microsatellite markers indicated that two closely related species, HC-A and HC-B, coexist along Kuroshio Current (Yasuda et al., 2004). Significant isolation resulting from geographic distance has been observed in these closely related species, and each population consists of either one or the other species (Yasuda et al., 2004). The two species have different reproductive timing, as indicated by sympatric populations of HC-A and HC-B. The brooding period of HC-A population seems to be different from sympatric HC-B population in southwest Japan (Saito et al., 2015) and the brooding period of HC-A is almost a month earlier than that of HC-B in the Philippines (Villanueva in review). Such ecological reproductive isolation mechanisms are considered to promote lineage sorting of the genes of the two *Heliopora* species.

Here, we examined intra- and interspecific sequence variation of ITS2, a nuclear microsatellite flanking region and *mtMutS* in HC-A and HC-B from geographically separated populations (approximately 1800 km apart, from the Philippines, Taiwan, and Japan) to determine whether the ITS2, microsatellite flanking region and *mtMutS* sequences can be used to detect species boundaries.

The goal of this study was to reveal genetic diversity of ITS2, a microsatellite flanking region and *mtMutS* in order to examine whether species boundaries of closely related octocorals are detectable by examining lineage sorting of the genes that are commonly used in phylogenetic analysis. Because the species boundary was originally detected through genetic admixture analysis using microsatellite data (Yasuda et al., 2004), we also sequenced a potentially neutral microsatellite flanking region for comparison with the commonly used markers described above.

## 2. Material and methods

### 2.1. Samples and laboratory experiments

#### 2.1.1. Samples and DNA extraction

The samples analyzed (Table 1) were collected from Japan, Taiwan, and the Philippines (maximum separation distance = approximately 1800 km) by either snorkeling or diving (Yasuda et al., 2004). Small fragments (1–2 cm) of each colony were collected and preserved in absolute ethanol. Genomic DNA was extracted using a DNeasy Blood & Tissue Kit (Qiagen).

#### 2.1.2. Intra-individual variation of ITS2 in HC-A and HC-B

Preliminary experiments revealed that direct sequencing of ITS2 is applicable to *H. coerulea*, of which >75% of individuals possess a single copy (i.e., no double peaks in the sequence chromatogram). However, intra-individual variation of ITS2 can present challenges for species identification and population genetic analysis that are comparable to those of a multi-gene family (Calderón et al., 2006; Escobar et al., 2012). Therefore, we also examined intragenomic variation among 16 individuals (nine HC-A and seven HC-B) by sequencing a total of 163 clones (3–16 clones per individual; Table 2) in order to verify comparisons of genetic diversity, species boundaries, and lineage sorting deduced from the directly sequenced data set. We used 5.8S–436 and 28S–663 primers developed by Aguilar and Sánchez (2007a,b) to amplify the ITS2 sequence. Thermocycling parameters were as follows: 3 min denaturation at 94 °C followed by 35 cycles of 30 s at 94 °C, 30 s at 52 °C, 30 s at 72 °C, with a final 5-min extension at 72 °C. Each PCR mixture (10 µL) consisted of 5 µL of KAPATaq HS ReadyMix with dye (Nippon Genetics), 0.7 µL of each primer (50 µM), 3.86 µL of double-distilled water, and 1 µL of template DNA. pGEM-T (Easy) Vector Systems (Promega) was used for cloning following the manufacturer's protocol. Inserts in the colonies were reamplified by PCR using M13 and U19 primers. One microliter of PCR product was cleaned using ExoSap-IT (Affymetrix) following manufacturer's protocol and then incubated at 37 °C for 15 min and 80 °C for 15 min. The cleaned PCR products were sequenced using M13 and U19 primers on an ABI 3130xl automated sequencer using BigDye ver. 3.1 terminator chemistry (Applied Biosystems, Foster City, CA). We manually checked sequencing errors using BioEdit ver. 7.0.9.0 (Hall, 1999) and then aligned all the sequences using GENETIX ver. 11.

#### 2.1.3. Direct sequencing of ITS2 for inter- and intraspecific identification

The main part of the analysis was based on the directly sequenced ITS2 dataset: the 226 sequenced ITS2 regions from *Heliopora* spp. (Table 1). Several double peaks appeared in the sequence chromatogram, making it difficult to determine haplotypes. We therefore subcloned and determined the corresponding haplotypes.

### 2.2. Sequencing the mtMutS region in HC-A and HC-B

Based on the mtMutS sequence of *H. coerulea* available from GenBank (accession number KC521415.1), we designed an original primer (HC-NDF-5', AAATGAGTCAAGTACCTATGCAG, HC-MutR 5', CCCCATAACTTCAATCTAGC), which amplified about 700 bp of the mtMutS region. Thermocycling parameters were as follows: 3 min denaturation at 94 °C followed by 35 cycles of 30 s at 94 °C, 30 s at 52 °C, 30 s at 72 °C, with a final 5-min extension at 72 °C. Each PCR mixture (10 µL) consisted of 5 µL of KAPATaq HS ReadyMix with dye (Nippon Genetics), 0.7 µL of each primer (50 µM), 3.86 µL of double-distilled water, and 1 µL of template

DNA. The PCR products were checked on agarose gels and then cleaned using ExoSap-IT (Affymetrix). One microliter of PCR product was cleaned using one unit of exonuclease and then incubated 37 °C for 15 min and at 80 °C for 15 min. The cleaned PCR products were sequenced on an ABI 3730xl automated sequencer using BigDye ver.3.1 terminator chemistry (Applied Biosystems) and M13 primer. We manually checked sequencing errors using BioEdit ver. 7.0.9.0 (Hall, 1999) and then aligned all the sequences using GENETIX ver. 11.

### 2.3. Sequencing of microsatellite flanking region

Genetic diversity and lineage sorting of a microsatellite flanking region, Saki08, was compared to that of ITS2 and mtDNA. Newly developed primers Saki08-332F 5'-ATTCTCTGGCACCACATTGA-3' and SSR compound primer CTCTCTCTCACACACACACACA were used to amplify the microsatellite flanking region (microsatellite locus Saki08, Yasuda et al. 2008). We chose the Saki08 locus because this locus had a long flanking region (310 bp). The microsatellite flanking region of 18 HC-A samples and 9 HC-B samples collected in Japan were cloned and sequenced. Thermocycling parameters were as follows: 3 min denaturation at 94 °C followed by 35 cycles of 30 s at 94 °C, 30 s at 60 °C, 30 s at 72 °C, with a final 5-min extension at 72 °C. Each PCR mixture (10 µL) consisted of 5 µL of KAPATaq HS ReadyMix with dye (Nippon Genetics), 0.7 µL of each primer (50 µM), 3.86 µL of double-distilled water, and 1 µL of template DNA. The pGEM-T (Easy) Vector Systems (Promega) was used for cloning the flanking region following the manufacturer's protocol. Inserts in 1–2 colonies per sample were reamplified by PCR using M13 and U19 primers. One microliter of PCR product was cleaned using one unit of exonuclease and then incubated at 37 °C for 15 min and 80 °C for 15 min. The cleaned PCR products were sequenced on an ABI 3130xl automated sequencer using BigDye ver.3.1 terminator chemistry (Applied Biosystems, Foster City, CA) with M13 or U19 primer. Primer sequences including microsatellite motif regions were excluded from analysis.

### 2.4. Genetic analysis of ITS2 and microsatellite flanking region sequences

To assess genetic diversity, the number of haplotypes ( $N_h$ ), number of polymorphic sites ( $N_p$ ), haplotype diversity ( $h$ ) (Nei, 1987), nucleotide diversity ( $\pi$ ), and mean number of pairwise differences between haplotypes ( $pd$ ) (Tajima, 1983) were calculated using DNASP ver. 5.1 (Librado and Rozas, 2009). Genetic diversity was calculated separately for direct sequencing and intra-genomic datasets.

A median-joining network (Bandelt et al., 1999) was constructed using NETWORK ver. 4.6.1.2 with the default settings in order to visualize evolutionary relationships between haplotypes obtained by direct sequencing and subcloning. We also constructed a maximum likelihood tree based on the 28 haplotypes found by direct sequencing using MEGA 6.0 (Tamura et al., 2013). The best model was estimated using MEGA 6.0 based on corrected Akaike Information Criteria. We used the Tamura–Nei 93 model (Tamura and Nei, 1993) for ITS2 and the Tamura–Nei 92 model with gamma distribution (Tamura, 1992) for the microsatellite flanking region to construct phylogenetic trees. Confidence values for phylogenetic trees were inferred using 1000 bootstrap replicates.

The secondary structures of ITS2 haplotypes were determined by comparison with previously reported structures (Aguilar and Sánchez, 2007a; McFadden et al., 2010). RNA sequences were submitted with constraints and restrictions that allowed folding according to the published secondary structures of octocoral ITS2 at 25 °C to MFOLD ver. 2.3 (Zuker, 2003). The structure with the

**Table 1**

Sampling sites and genetic diversity of ITS2 by direct sequence and 6 microsatellite loci in *Heliopora* sp. HO: Observed heterozygosity, HE: Expected heterozygosity, Nind: number of individuals, Nseq: number of sequences, Nh: number of haplotypes, Np: number of polymorphic sites,  $\pi$ : nucleotide diversity, h: haplotype diversity. Na: mean number of alleles, Ho: observed heterozygosity, He: expected heterozygosity, F: inbreeding coefficient. Subtotal, total or average values are shown in bold.

| Inter population and inter species diversity |                      |                                 |       |           |                              | mtMtuS    |            | ITS2 (direct sequence) |           |           |               |              | Mirrosatellite flanking region |           |           |           |              | 6 Microsatellite loci |            |             |             |             |              |
|--|----------------------|---------------------------------|-------|-----------|------------------------------|-----------|------------|------------------------|-----------|-----------|---------------|--------------|--------------------------------|-----------|-----------|-----------|--------------|-----------------------|------------|-------------|-------------|-------------|--------------|
| Country                                      | Region               | Collection site                 | Abbr. | Depth (m) | Coordinates                  | N         | Nind       | Nseq                   | Nh        | Np        | $\pi$         | h            | Nind                           | Nseq      | Nh        | Np        | $\pi$        | h                     | major spp. | Na          | Ho          | He          | F            |
| Japan  | Amami Oshima         | Sankaku Iwa                     | AMM   | 6–9       | 28°7'2.53"N 129°21'49.69"E   | 24        | 26         | 4                      | 3         | 0.0011    | 0.222         |              |                                |           |           |           |              |                       | A          | 5.43        | 0.685       | 0.553       | –0.238       |
|  | Yaeyama              | Iriomote-north                  | IRI   | 3.9–8.5   | 24°24'5.50"N 123°53'21.70"E  | 3         | 15         | 15                     | 1         | 0         | 0.0000        | 0.000        | 8                              | 13        | 5         | 4         | 0.004        | 0.628                 | A          | 6.00        | 0.743       | 0.683       | –0.088       |
|  |                      | Yonara West                     | SENA  | 1.5–8.6   | 24°21'40.10"N 123°56'53.50"E | 5         | 14         | 14                     | 1         | 0         | 0.0000        | 0.000        | 10                             | 19        | 8         | 6         | 0.005        | 0.842                 | A          | 5.43        | 0.673       | 0.661       | –0.019       |
| Taiwan                                       | Taiwan               | Kenting Park-Little Bay         | TWNA  | 2.8–4.7   | 21°59'43.29"N 120°42'18.96"E | 5         | 10         | 10                     | 1         | 0         | 0.0000        | 0.000        |                                |           |           |           |              |                       | A          | 4.14        | 0.529       | 0.594       | 0.110        |
|  |                      | Kenting Park-Chanfan Rock       | TWNB  | 9.6–11.4  | 21°56'1.07"N 120°49'19.19"E  | 8         | 10         | 10                     | 2         | 1         | 0.0024        | 0.533        |                                |           |           |           |              |                       | A          | 4.00        | 0.614       | 0.645       | 0.048        |
| Philippines                                  | Verde Island Passage | Lian-Coral Beach Club beach     | VCALA | 1–4.7     | 13°58'53.79"N 120°37'45.34"E | 11        | 11         | 1                      | 0         | 0.0000    | 0.000         |              |                                |           |           |           |              |                       | A          | 5.71        | 0.774       | 0.685       | –0.130       |
|  |                      | Lian-Talin Point                | VCALB | 3.7–4.7   | 14°02'07.70"N 120°36'42.30"E | 7         | 8          | 2                      | 1         | 0.0011    | 0.250         |              |                                |           |           |           |              |                       | A          | 4.43        | 0.735       | 0.647       | –0.136       |
|  |                      | <b>Subtotal or average in A</b> |       |           |                              | <b>21</b> | <b>91</b>  | <b>94</b>              | <b>5</b>  | <b>4</b>  | <b>0.0008</b> | <b>0.162</b> | <b>18</b>                      | <b>32</b> | <b>10</b> | <b>8</b>  | <b>0.004</b> | <b>0.796</b>          |            | <b>5.02</b> | <b>0.68</b> | <b>0.64</b> | <b>–0.06</b> |
| Japan  | Yaeyama              | Shiraho reef                    | SHIR  | 0–2       | 24°21'47.00"N 124°15'19.10"E | 12        | 28         | 34                     | 4         | 6         | 0.0097        | 0.401        | 7                              | 13        | 3         | 2         | 0.003        | 0.590                 | B          | 3.29        | 0.622       | 0.550       | –0.132       |
|  |                      | Sekisei-Kengu                   | SESA  | 1.8–5.4   | 24°13'24.50"N 124° 1'44.90"E | 2         | 20         | 32                     | 10        | 7         | 0.0104        | 0.559        | 1                              | 2         | 1         | 0         |              |                       | B          | 3.29        | 0.429       | 0.430       | 0.004        |
|  |                      | Sekisei-East1                   | SESB  | 4–10      | 24°15'31.20"N 124° 7'51.20"E | 2         | 20         | 38                     | 10        | 6         | 0.0140        | 0.720        |                                |           |           |           |              |                       | B          | 2.71        | 0.593       | 0.481       | –0.234       |
|  |                      | Sekisei-East2                   | SESC  | 1.7–9.9   | 24°17'15.10"N 124° 8'58.60"E | 2         | 4          | 4                      | 1         | 0         | 0.0000        | 0.000        |                                |           |           |           |              |                       | B          | 2.57        | 0.607       | 0.505       | –0.202       |
|  |                      | Sekisei-South                   | SESE  | 2.2–8.7   | 24°19'13.40"N 124° 9'46.10"E | 20        | 33         | 6                      | 7         | 0.0141    | 0.665         | 1            | 2                              | 2         | 2         | 0.006     | 1.000        | B                     | 2.57       | 0.493       | 0.384       | –0.285      |              |
| Philippines                                  | Verde Island Passage | Caban-Saddel                    | VCABA | 2.5–6.8   | 13°41'7.29"N 120°50'23.12"E  | 13        | 15         | 4                      | 7         | 0.0064    | 0.371         |              |                                |           |           |           |              | B                     | 2.57       | 0.396       | 0.313       | –0.266      |              |
|  |                      | Caban-Dari laot                 | VCABB | 4.4–6.6   | 13°41'24.17"N 120°50'28.66"E | 6         | 7          | 2                      | 6         | 0.0078    | 0.286         |              |                                |           |           |           |              | B                     | 2.86       | 0.595       | 0.470       | –0.267      |              |
|  |                      | Maricaban-Dulo                  | VMARA | 2.5–6.5   | 13°37'51.46"N 120°58'19.96"E | 3         | 5          | 4                      | 7         | 0.0183    | 0.900         |              |                                |           |           |           |              | B                     | 1.43       | 0.429       | 0.257       | –0.667      |              |
|  |                      | Maricaban-Site 3                | VMARB | 2.5–3.2   | 13°38'38.36"N 120°57'10.50"E | 9         | 10         | 2                      | 7         | 0.0064    | 0.200         |              |                                |           |           |           |              | B                     | 2.71       | 0.508       | 0.531       | 0.044       |              |
|  |                      | Anilao-Arthur's Rock            | VBAT  | 4.1–10.7  | 13°43'52.84"N 120°52'1.98"E  | 10        | 10         | 2                      | 1         | 0.0009    | 0.200         |              |                                |           |           |           |              | B                     | 2.71       | 0.514       | 0.473       | –0.087      |              |
|  |                      | Puerto Galera-Giant Clam Garden | VPUE  | 1.4–11    | 13°30'52.71"N 120°57'8.14"E  | 2         | 2          | 1                      | 0         | 0.0000    | 0.000         |              |                                |           |           |           |              | B                     | 1.86       | 0.429       | 0.405       | –0.059      |              |
|  |                      | <b>Subtotal or average in B</b> |       |           |                              | <b>18</b> | <b>135</b> | <b>190</b>             | <b>23</b> | <b>12</b> | <b>0.0140</b> | <b>0.669</b> | <b>9</b>                       | <b>17</b> | <b>5</b>  | <b>3</b>  | <b>0.004</b> | <b>0.735</b>          |            | <b>2.60</b> | <b>0.51</b> | <b>0.44</b> | <b>–0.20</b> |
|  |                      | <b>A + B Total</b>              |       |           |                              | <b>39</b> | <b>226</b> | <b>284</b>             | <b>28</b> | <b>16</b> | <b>0.015</b>  | <b>0.761</b> | <b>27</b>                      | <b>49</b> | <b>14</b> | <b>10</b> | <b>0.005</b> | <b>0.863</b>          |            |             |             |             |              |

**Table 2**

Intra- and inter-individual genetic diversity of ITS2 estimated by subcloning, Nind: number of individuals, Nseq: number of sequences, Nc: number of clones sequenced. Nh: mean number of alleles Np: number of polymorphic sites, h: haplotype diversity,  $\pi$ : nucleotide diversity. Nmis: number of sequences that are only found by subcloning methods and not by direct sequencing. Unique bases: unique point substitution found in individuals (possible artificial errors). Subtotal, total or average values are shown in bold.

| ID       | Pop  | spp.               | Intra-genomic diversity recovered from subcloning |           |           |              |               |           |             | 73rd nucleotide |           |                   |
|----------|------|--------------------|---|-----------|-----------|--------------|---------------|-----------|-------------|-----------------|-----------|-------------------|
|          |      |                    | Nc  | Nh        | Np        | h            | $\pi$         | Nmis      | % Nmis      | Thymine         | Cytosine  | Unique bases (bp) |
| SENA01   | SENA | A                  | 13  | 3         | 2         | 0.295        | 0.0014        | 2         | 15.4        | 13              | 0         | 2                 |
| SENA03   | SENA | A                  | 9   | 1         | 0         | 0.000        | 0.0000        | 0         | 0.0         | 9               | 0         | 0                 |
| SENA04   | SENA | A                  | 3   | 1         | 0         | 0.000        | 0.0000        | 0         | 0.0         | 3               | 0         | 0                 |
| SENA06   | SENA | A                  | 14  | 2         | 1         | 0.143        | 0.0007        | 1         | 7.1         | 14              | 0         | 1                 |
| SENA07   | SENA | A                  | 5   | 2         | 1         | 0.400        | 0.0018        | 1         | 20.0        | 5               | 0         | 1                 |
| SENA08   | SENA | A                  | 13  | 2         | 5         | 0.154        | 0.0035        | 1         | 7.7         | 13              | 0         | 5                 |
| SENA09   | SENA | A                  | 16  | 3         | 15        | 0.242        | 0.0105        | 2         | 12.5        | 14              | 2         | 13                |
| SENA10   | SENA | A                  | 10  | 2         | 11        | 0.200        | 0.0101        | 1         | 10.0        | 10              | 0         | 11                |
| SENA12   | SENA | A                  | 14  | 1         | 0         | 0.000        | 0.0000        | 0         | 0.0         | 14              | 0         | 0                 |
| <b>9</b> |      | <b>A all</b>       | <b>97</b>   | <b>9</b>  | <b>24</b> | <b>0.159</b> | <b>0.0036</b> | <b>8</b>  | <b>8.2</b>  | <b>95</b>       | <b>2</b>  | <b>33</b>         |
| SESA01   | SESA | B                  | 14  | 10        | 12        | 0.945        | 0.0126        | 6         | 42.9        | 0               | 14        | 4                 |
| SESA02   | SESA | B                  | 10  | 6         | 10        | 0.778        | 0.0164        | 5         | 50.0        | 0               | 10        | 4                 |
| SESA03   | SESA | B                  | 3   | 1         | 0         | 0.000        | 0.0000        | 0         | 0.0         | 0               | 3         | 0                 |
| SESA04   | SESA | B                  | 13  | 4         | 10        | 0.423        | 0.0094        | 1         | 7.7         | 0               | 8         | 1                 |
| SESA08   | SESA | B                  | 3   | 1         | 0         | 0.000        | 0.0000        | 0         | 0.0         | 0               | 3         | 0                 |
| SESA10   | SESA | B                  | 13  | 6         | 8         | 0.718        | 0.0164        | 5         | 38.5        | 0               | 13        | 2                 |
| SESA11   | SESA | B                  | 10  | 2         | 1         | 0.200        | 0.0009        | 1         | 10.0        | 0               | 10        | 1                 |
| <b>7</b> |      | <b>B all</b>       | <b>66</b>   | <b>21</b> | <b>23</b> | <b>0.633</b> | <b>0.0097</b> | <b>18</b> | <b>29.0</b> | <b>0</b>        | <b>62</b> | <b>12</b>         |
|          |      | <b>A + B total</b> | <b>163</b>  | <b>30</b> | <b>42</b> | <b>0.644</b> | <b>0.0084</b> | <b>26</b> | <b>16.0</b> | <b>95</b>       | <b>64</b> | <b>45</b>         |

greatest negative free energy with conserved ITS2 ring structure was confirmed by comparison with previously published secondary structures (Aguilar and Sánchez, 2007a).

### 2.5. Genotyping analysis of microsatellite loci

We used data from individuals that we previously genotyped using six unlinked microsatellite loci for microsatellite analysis (Yasuda et al., 2004). The neutrality of each locus was confirmed in each species using LOSITAN software (Antao et al., 2008) based on the infinite alleles model (IAM) and the stepwise mutation model (SMM). LOSITAN performs  $F_{ST}$ -outlier analysis to identify microsatellite loci under selection. The same individuals for which ITS2 were sequenced were analyzed again for comparison. The genetic diversity of each microsatellite locus, the effective number of alleles, and observed and expected heterozygosities were estimated using GenAEx ver. 6.41 (Peakall and Smouse, 2005).

STRUCTURE software (Pritchard et al., 2000) ver. 2.3.4 was used to infer individual species (HC-A and HC-B). An admixture model without a priori information was used to assign species by inferring a hypothetical genetic cluster; such tests can be used to reveal cryptic *Heliopora* species (Yasuda et al., 2004). Ten independent runs with different seed numbers were calculated at  $K=2$  with 100,000 burn-ins and 200,000 Markov chain Monte Carlo (MCMC) iterations to confirm consistency of the results. Bar plots were generated by CLUMPP software (Jakobsson and Rosenberg, 2007).

To examine population demography, BOTTLENECK ver. 1.2.02 (Piry et al., 1999) was used to detect bottlenecks using two common approaches: detection of transient heterozygosity excess and a mode-shift indicator of allele frequencies. Heterozygosity excess was detected using the one-tailed Wilcoxon sign test, which is the best method for studies using fewer than 20 loci (Piry et al., 1999). This test was conducted with a two-phase model (TPM) that included 95% single-step mutations and 5% multiple-step mutations as recommended by Piry et al., 1999. The mode-shift indicator we used is a descriptor of the allele frequency distribution that discriminates bottlenecked populations from stable populations (Luikart et al., 1998).

## 3. Results and discussions

### 3.1. Genetic diversity and lineage sorting of ITS2 and microsatellite flanking region: implication for species delimitation based on phylogenetic analysis

STRUCTURE analysis using microsatellite loci indicated that 89 individuals from seven populations belonged to HC-A, and 137 individuals from 11 populations belonged to HC-B (Fig. 1). All individuals were assigned (>75%) to one of the two species. Each population used in this study consisted of a single species, except for IRI and VCALA, both of which contained an individual of a different species (Fig. 1).

Of the 226 individuals for which we directly sequenced ITS2, approximately 74% (168 sequences) showed no double peaks (single-haplotype individuals). The total sequence length of ITS2 used for the analysis was 219 bp without any insertions or deletions. This result was consistent with previous reports that direct ITS2 sequencing has been successful for some octocorals (Aguilar and Sánchez, 2007a,b; Grajales et al., 2007) and other corals (Marquez et al., 2003; Chen et al., 2004; Wei et al., 2006).

Direct sequencing and subcloning methods using the same individuals recovered the same dominant ITS2 haplotypes in each individual. However, subcloning sometimes revealed more ITS2 haplotype variation within individuals than we expected from direct sequencing, possibly due to the presence of minor ITS2 haplotypes (Table 2, Fig. 2). There were a total of 42 polymorphic sites with 30 haplotypes and 22 singletons (a haplotype that was found once) in the subcloned dataset (Fig. 2a). Some ITS2 haplotypes (8.2% in HC-A and 29% in HC-B) were found only by subcloning methods and not by direct sequencing of the same individual (Table 2; Fig. 2b). We used the same protocol for subcloning HC-A and HC-B, so we can assume that artificial error rates that occurred during PCR, subcloning, and sequencing are comparable between the two species. Therefore, it is likely that HC-B has more minor intraindividual variation, such as low-frequency haplotypes or pseudogenes of ITS2 than does HC-A. HC-A has overall lower genetic diversity, and only two individuals from HC-A (SENA09, 10) contained any distinct sequences (Fig. 2a). The secondary structure estimated for these sequences was the same as Hap\_5

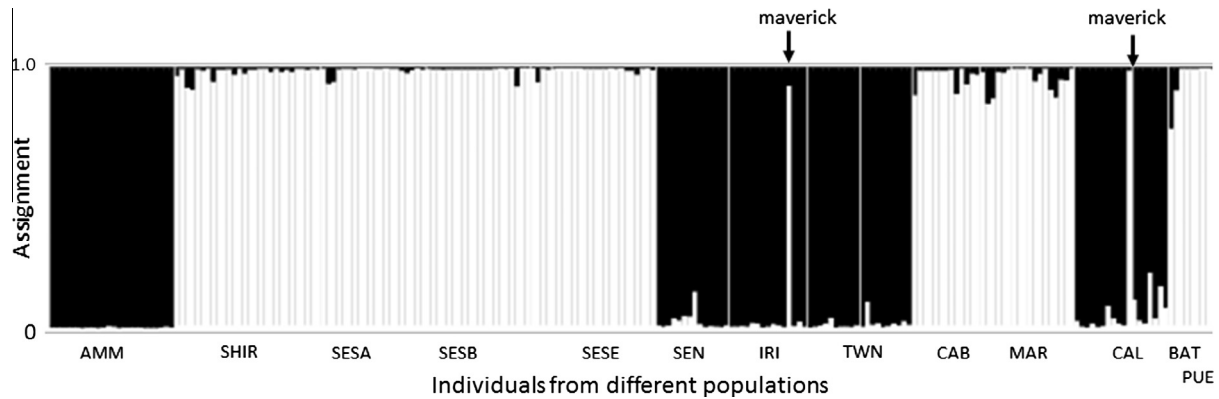


**Fig. 1.** Assignment test to infer species (HC-A in black and HC-B in white) using STRUCTURE analysis ( $K = 2$ ). X-axis shows each individual; y-axis shows the proportion of assigned hypothetical clusters. Arrows indicate "mavericks" that had Hap\_1. Numbers indicate mutational steps between haplotypes.

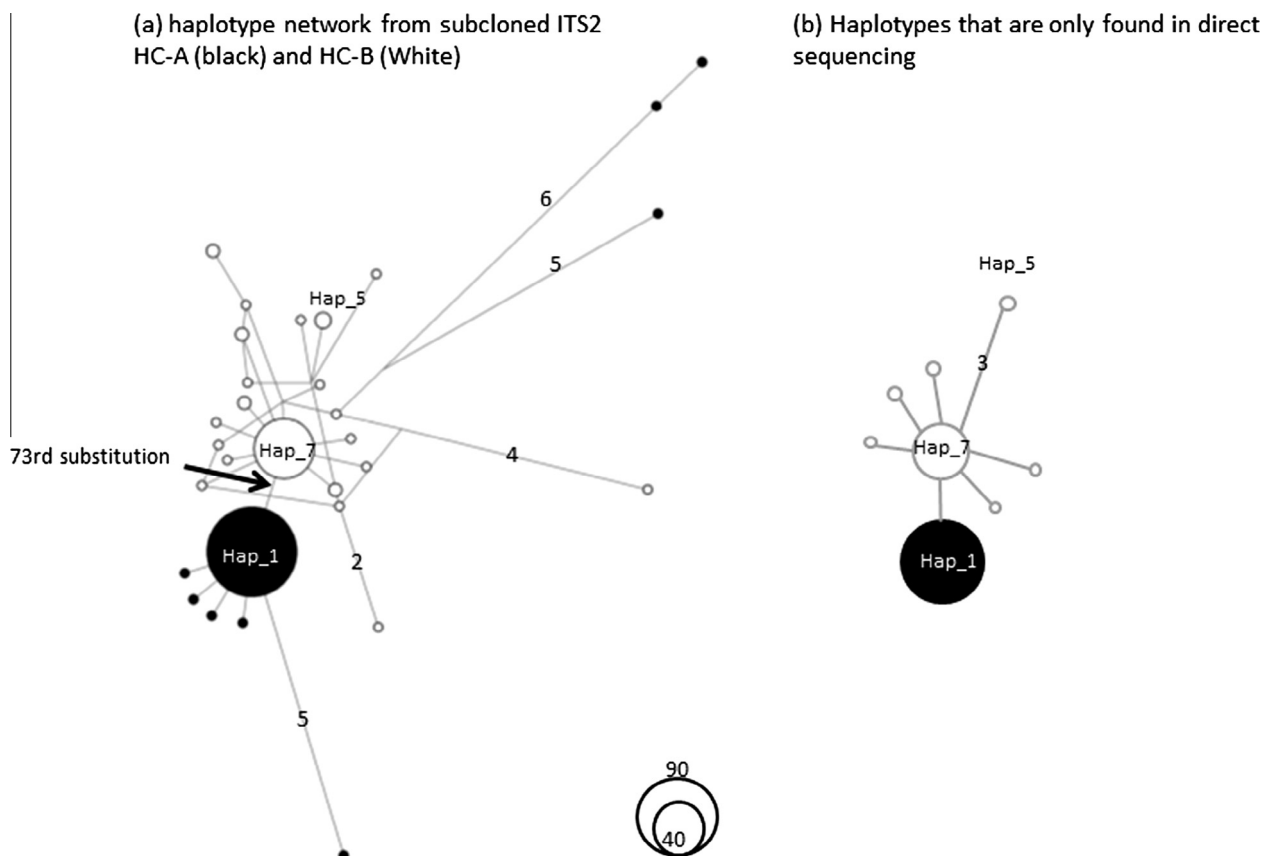


**Fig. 2.** Intragenomic ITS2 variation illustrated using median-joining network of each species. (a) HC-A (97 sequences from nine individuals shown in black) and HC-B (66 sequences from seven individuals shown in white). The arrow indicates the location of the 73rd substitution in the haplotype network. (b) Haplotypes that were only found by direct sequencing.

(Fig. 3b), but with lower negative free energy ( $-77.3$  kcal). This indicates that these sequences have less stable secondary structures than the dominant haplotypes, even if they are not pseudogenes. These sequences are not detectable in the sequence chromatograms of direct sequencing, so their relative frequency in the genome is considered to be very low relative to the dominant haplotypes. Previous studies have shown that bacterial cloning of multi-copy genes overestimates genetic diversity (LaJeunesse and Pinzón, 2007; Thornhill et al., 2007). However, both direct sequencing and subcloning indicated higher intraindividual genetic diversity in HC-B than in HC-A, and overall lineage

sorting between HC-A and HC-B with a point mutation that separates the two species (>99% of the individuals analyzed did not share haplotypes between species). Although genetic diversity might be underestimated by ignoring minor intraindividual variations that are only detectable by cloning, subsequent analyses were based on the dataset obtained from direct sequencing in which 28 haplotypes with 16 polymorphic sites and six singletons were uncovered.

HC-A included five haplotypes (Hap\_1–4, 10), and HC-B included 23 haplotypes (Hap\_5–9, 11–28), although two HC-B individuals had Hap\_1 (Fig. 3). In HC-A, the most dominant

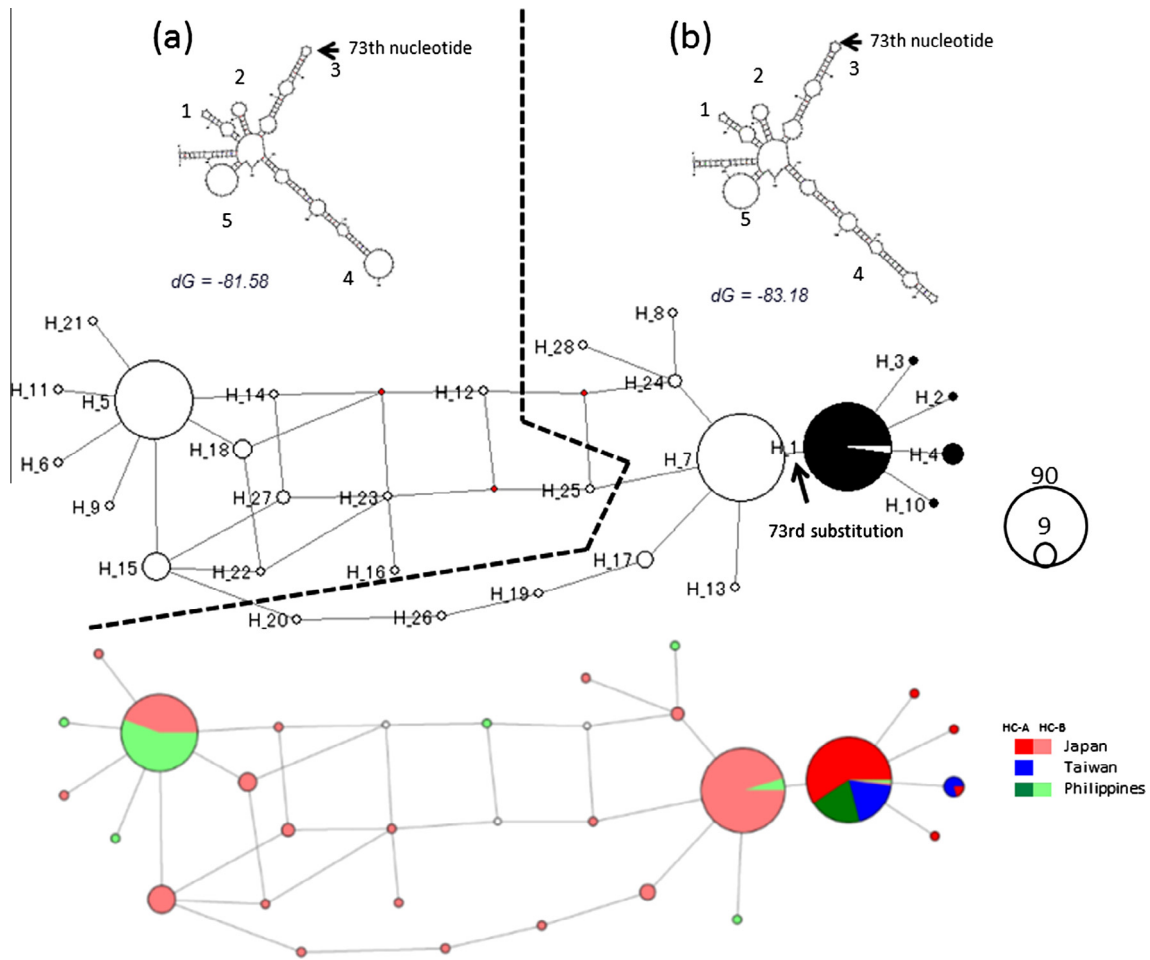


**Fig. 3.** Median-joining network based on ITS2 sequences and their secondary structures. All haplotypes (H<sub>1</sub>–H<sub>28</sub>) and median vectors were connected by a substitution. HC-A individuals are shown in black and HC-B individuals are shown in white. The position of the mutation that separates the two species (between Hap 1 and Hap 7) is shown by an arrow in the black and white network. Dashed line separates haplotype groups that have slightly different secondary structures (the tip of helix 4) (a) and (b). A network that includes geographic information is shown at the bottom of the figure.

haplotype was Hap<sub>1</sub>; two codominant, possibly ancestral haplotypes in HC-B were Hap<sub>5</sub> and Hap<sub>7</sub>. The only shared haplotype between the species was Hap<sub>1</sub>, which was found in two individuals determined to be HC-B by microsatellite analysis (Figs. 1 and 3). Both HC-B individuals were “mavericks” in HC-A-dominant populations (IRI and VCALA), as determined by microsatellite analysis (Fig. 1). Microsatellite data for a few individuals in a previous study showed possible hybrid patterns (Yasuda et al., 2004). This may have been caused by introgression associated with historical hybridization or by incomplete lineage sorting. Nonetheless, overall lineage sorting of ITS2 was observed between species (<1% of HC-A and HC-B individuals shared haplotypes) indicating restricted gene flow between the two species. We thus used ITS2 data to confirm the restricted gene flow between HC-A and HC-B that was previously indicated by microsatellite loci data. It is empirically possible to identify HC-A and HC-B with high accuracy (99.1% by direct sequencing and 98.8% by subcloning) by examining the fixed mutation at the 73rd position after DNA barcoding using ITS2. Phylogenetic trees indicated paraphyly, not a reciprocal monophyly for HC-A and HC-B (Fig. 4). This suggests that determining *Heliopora* spp. species boundaries using phylogenetic trees based on ITS2 sequences without any prior information is difficult.

The 310 bp of microsatellite flanking region we sequenced, excluding the primer site and compound microsatellite repeat region, indicated no insertions or deletions among 49 sequences. There were fourteen haplotypes with 10 polymorphic sites and

seven singletons. Unlike the ITS2 sequences, genetic diversity of the possibly neutral microsatellite flanking region was comparable in the two species ( $\pi$  and  $h$ ) (Table 1).

The haplotype network deduced from the microsatellite flanking region indicated only one haplotype (H<sub>3</sub>) was shared between HC-A and HC-B (Fig. 5a). Because H<sub>3</sub> is the most dominant haplotype, it is likely that the ancestral haplotype is still shared between the two species. This implies incomplete lineage sorting rather than hybridization. The maximum likelihood phylogenetic tree did not show reciprocal monophyly or even paraphyly (Fig. 5b). The H<sub>3</sub> haplotype was more frequently shared between species in the microsatellite flanking region than in ITS2, indicating that the ITS2 gene evolved more rapidly than the possibly neutral microsatellite flanking region (Saki 08). In this regard, ITS2 is considered to be a more informative locus in terms of species delimitation than other neutral nuclear regions, such as microsatellite flanking regions. However, caution is required when using ITS2 for species delimitation based on reciprocal monophyly in phylogenetic analyses because, as this study showed, not all closely related octocoral species show reciprocal monophyly.

The intraindividual genetic diversity of ITS2 that we found after subcloning poses another problem for phylogenetic studies. It is difficult to identify all intraindividual ITS2 diversity using direct sequencing or subcloning, which could result in underestimation or overestimation of genetic diversity, respectively. Although we could not use Denaturing Gradient Gel Electrophoresis (DGGE)



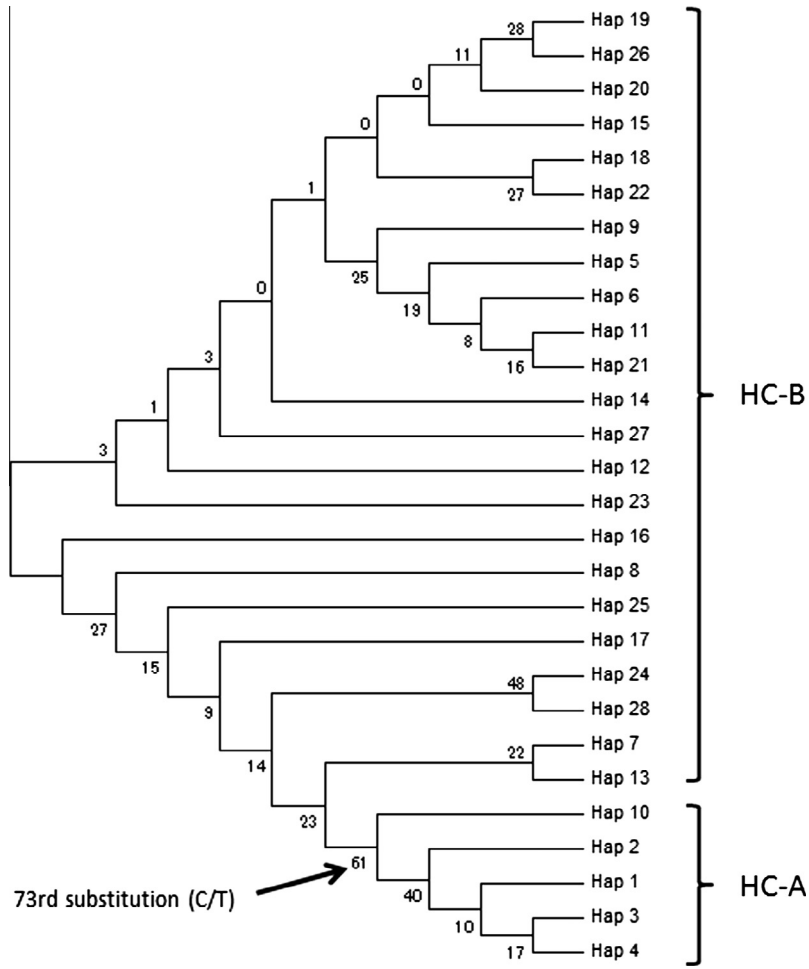


**Fig. 4.** Maximum likelihood tree reconstructed using 28 haplotype sequences of ITS2 from two *Heliopora* spp. (HC-A and HC-B) obtained from 226 individuals by direct sequencing. Numbers indicate bootstrap values.

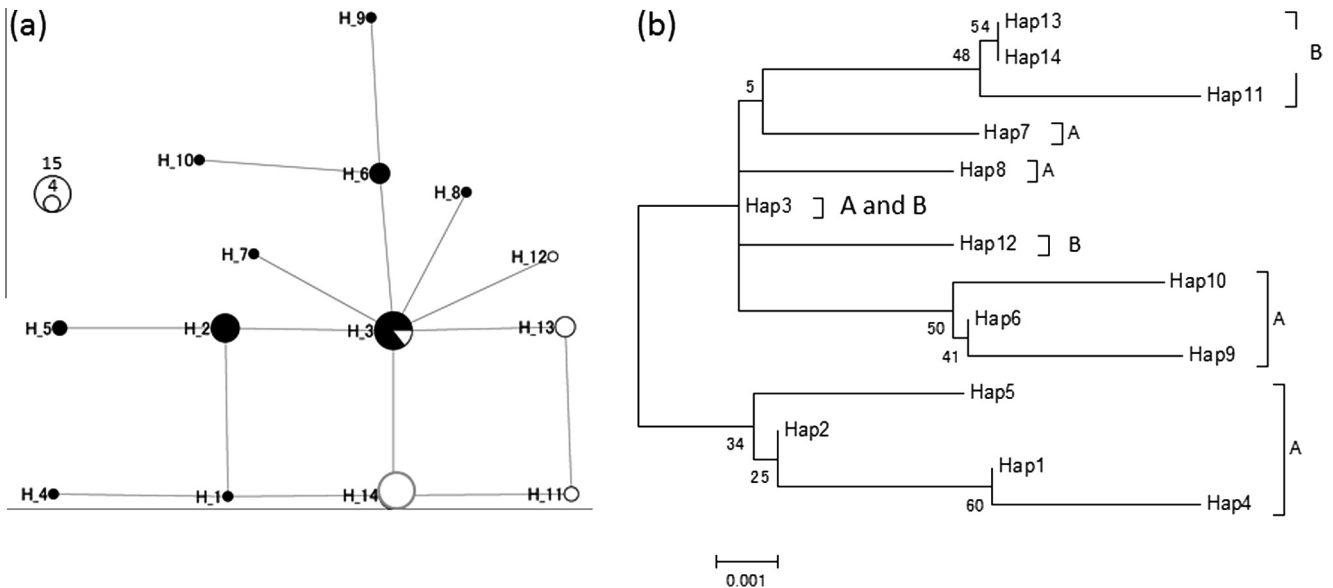


**Fig. 5.** (a) Median-joining network and (b) maximum likelihood tree based on microsatellite flanking sequences. HC-A individuals are shown in black and HC-B individuals are shown in white and all haplotypes are connected by a substitution in (a). Numbers in (b) indicate bootstrap values.

here, DGGE methods are reported to be useful for detecting intraindividual variation of ITS2 and for avoiding the miscalculation of genetic diversity that can be caused by subcloning (Lajeunesse and Pinzón, 2007; Torres-Suarez, 2014).

### 3.2. Differences in genetic diversity of HC-A and HC-B in ITS2

Both the direct sequencing and subcloned sequence datasets of ITS2 indicated that genetic diversity of ITS2 in HC-A was considerably lower than that in HC-B (Tables 1 and 2). Haplotype diversity, as determined by direct sequencing, was approximately fourfold higher, and  $\pi$  was approximately 18-fold higher, in HC-B than in HC-A. Similarly, subcloned sequencing data indicated that  $h$  was approximately fourfold higher, and  $\pi$  was approximately threefold higher, in HC-B than HC-A (Tables 1 and 2). This indicates higher intragenomic and intraspecific genetic diversity in HC-B ITS2 than in HC-A ITS2. This contrasts with possibly neutral microsatellite flanking region (*Saki 08*) analysis and microsatellite genotyping analysis using 6 loci. These analyses showed comparable genetic diversity between HC-A and HC-B.

Four hypothesis were considered: (1) HC-A is a relatively young species and still has low genetic diversity; (2) HC-A demographic history includes a population bottleneck; (3) selection specific to the ITS2 sequence has resulted in lower genetic diversity in HC-A; and (4) the rate of concerted evolution is faster in HC-A than in HC-B. We consider the first two hypotheses to be unlikely because HC-A shows somewhat higher or comparative genetic diversity in microsatellite loci relative to HC-B (Table 1). Bottleneck analysis using microsatellite loci indicated a possible bottleneck in four populations of HC-B (SESB, SESE, VMAR, and VBAT) and in only one HC-A population (SENA) (Wilcoxon and mode-shift tests were significant at  $P < 0.05$ ). Therefore, it is unlikely that a population bottleneck specific to HC-A resulted in the observed low genetic diversity. We consider the third and fourth hypotheses to be most likely. According to the outlier  $F_{ST}$  analysis, the six microsatellite loci used in this study, including the sequenced *Saki08*, were neutral in each species and were probably not under selection; therefore, if any selection pressure exists on a genetic marker, it is more likely to be on ITS2 than on one of the microsatellite loci. HC-A and HC-B are distributed in different environments. HC-A often appears in relatively open environments, such as reef slopes, while HC-B often appears in semi-closed environments, such as inside reefs (Yasuda et al., 2004, 2010). Accumulated evidence from recent studies suggests that variations in rDNA are associated with fitness and the evolutionary ecology of organisms and may be significantly correlated with important environmental factors (Weider et al., 2005). Therefore, environmental factors may be associated with the genetic diversity of ITS2. It is also likely that the species-specific rate of concerted evolution is faster in HC-A than in HC-B. If the rate of concerted evolution is fast enough, intraindividual genetic diversity of some genes may be low enough to make them better species markers than other neutral nuclear loci. However, if the rate of concerted evolution is slow, relatively high intraindividual genetic diversity may hinder species identification. The relatively high intraindividual variation in HC-B implies relatively slow concerted evolution in that species. Fixation of variants in a population by molecular drive is caused by stochastic and directional processes of family turnover (Dover, 1982). HC-A may have a faster rate of concerted evolution than HC-B. It is also possible that the relatively high genetic diversity of HC-B resulted from a slow rate of concerted evolution associated with balancing selection caused by environmental factors, whereas the relatively low genetic diversity of HC-A resulted from relatively rapid concerted evolution associated with directional selection. Simulations and theory suggest that a single mutation can be fixed in a relatively short time period during concerted

evolution (Birky and Skavaril, 1976), but there are no reports indicating that rates of concerted evolution differ greatly between sibling species. Therefore, more evidence is needed to attribute the observed difference in genetic diversity between species to concerted evolution.

This study suggests that genetic diversity and, possibly, the rate of concerted evolution may differ between very closely related octocoral species. Therefore, sequencing of multiple individuals and examination of intraindividual diversity using DGGE is recommended when examining genetic diversity of ITS2 (Lajeunesse, and Pinzón, 2007).

### 3.3. Secondary structure of ITS2 and species delimitation

The secondary structure of ITS2 exhibited the highly conserved six-helicoidal ring-model structure (Fig. 3) that has been previously reported (Aguilar and Sánchez 2007a,b; McFadden et al., 2010). Interestingly, there was only one base-pair substitution between HC-A (Hap\_1) and HC-B (Hap\_7) that was not related to secondary structure or CBCs. The point mutation that discriminates the species (between Hap\_1 and Hap\_7) occurred at the 73rd nucleotide (thymine in HC-A and cytosine in HC-B), which corresponds to the tip of helix 3 (Fig. 3). Two major secondary structures that differed slightly at the tip of helix 4 were found within HC-B (Fig. 3). However, these structures are not likely associated with reproductive isolation, as 25 individuals appeared to have both Hap\_5 and Hap\_7 in the heterozygous state. A greater abundance of Hap\_7 was found in Japanese HC-B than in HC-B from the Philippines, whereas Hap\_5 was more abundant in the HC-B populations from the Philippines than in those from Japan (Fig. 3). Species-specific secondary structures have been reported in gorgonian species (Aguilar and Sánchez, 2007a,b). CBCs in ITS2 secondary structures are strongly correlated with distinct biological species (Coleman and Vacquier, 2002) and the absence of CBCs indicates >75% probability that individuals are from the same species (Muller et al., 2007). More recently, Torres-Suarez (2014) found that the presence of CBCs and hemi-CBCs was useful for differentiating between octocoral species and populations. In this context, it is notable that the point mutation that discriminated the closely related *Heliopora* spp. was not related to secondary structure or CBCs.

### 3.4. Genetic diversity of *mtMutS*

The 699 bp *mtMutS* sequences were identical among 39 individuals (18 HC-A and 21 HC-B) collected from eight populations (Table 1), indicating that the mutation rate of *mtMutS* is too slow to detect recent speciation of *Heliopora*. The relatively small genetic diversity in mtDNA could be also explained by bottleneck and founder effects that resulted in a small effective mtDNA population size. However, there was almost no sign of a bottleneck in the nuclear microsatellite loci, implying that invariant mtDNA is not likely caused by a bottleneck. Although the *mtMutS* gene has higher rates of mutation than other octocoral genes (Bilewicz and Degnan, 2011), mtDNA of anthozoans generally evolves very slowly (France et al., 1996; van Oppen et al., 1999), and sometimes mtDNA sequences of corals are identical among different genera or even families (Fukami et al., 2004; Romano and Palumbi, 1996). *MtMutS* is too conservative for population genetic analysis, species delimitation, or phylogenetic analysis in closely related *Heliopora* spp. Although *mtMutS* provides excellent resolution for discriminating among closely related octocoral taxa (e.g. McFadden et al., 2011), the present study suggests that *mtMutS* may sometimes fail to detect boundaries between closely related octocoral species.

#### 4. Conclusions

Fewer ITS2 haplotypes were shared between HC-A and HC-B than were haplotypes of a neutral, single copy microsatellite gene. This is likely due to natural selection and/or concerted evolution that promoted lineage sorting. Because the rate of concerted evolution of ITS2 may differ greatly between closely related species, we recommend the sequencing of multiple individuals for phylogenetic studies in order to examine genetic diversity of ITS2. Although fixed mutation of ITS2 indicated restricted gene flow between two *Heliopora* spp., a phylogenetic tree showed paraphyly and not reciprocal monophyly. Neither CBCs nor secondary structure was related to the boundary between species. Due to its highly conserved sequence, *mtMutS* cannot be used to detect the boundary between closely related *Heliopora* spp. Our data suggest that caution is warranted when reciprocal monophyly is used as the criterion to delimit closely related octocoral species in phylogenetic trees based on ITS2 or *mtMutS* sequences and that detection of the precise species boundary requires genetic admixture analysis based on multiple loci and individuals.

#### Acknowledgments

We appreciate the assistance of H. Shimohigashi with obtaining some of the sequence data. We thank Mr. T. Nagata at the incorporated foundation Okinawa Prefecture Environment Science Centre for sampling specimens. This study was funded by the Collaborative Research of Tropical Biosphere Research Center, University of the Ryukyus and by Environment Research, Technology Development Fund of the Ministry of the Environment, Japan (4-1304), and the Research Institute of Marine Invertebrates, (Tokyo).

This work was financially supported by the Program to Disseminate Tenure Tracking System from the Ministry of Education, Culture, Sports, Science and Technology (MEXT).

#### References

- Aguilar, C., Sánchez, J., 2007a. Phylogenetic hypotheses of gorgoniid octocorals according to ITS2 and their predicted RNA secondary structures. *Mol. Phylogenet. Evol.* 43, 774–786.
- Aguilar, C., Sánchez, J.A., 2007b. Molecular morphometrics: contribution of ITS2 sequences and predicted RNA secondary structures to octocoral systematics. *B. Mar. Sci.* 81, 335–349.
- Antao, T., Lopes, A., Lopes, R., Beja-Pereira, A., Luikart, G., 2008. LOSITAN: A workbench to detect molecular adaptation based on a *Fst*-outlier method. *BMC Bioinformatics* 9, 323.
- Bandelt, H.J., Forster, P., Röhl, A., 1999. Median-joining networks for inferring intraspecific phylogenies. *Mol. Biol. Evol.* 16, 37–48.
- Bayer, F., 1961. The Shallow-Water Octocorallia of the West Indian Region. A Manual for marine biologists, p. 373.
- Bilewicz, J., Degnan, S., 2011. A unique horizontal gene transfer event has provided the octocoral mitochondrial genome with an active mismatch repair gene that has potential for an unusual self-contained function. *BMC Evol. Biol.* 11, 228.
- Birky Jr., C.W., Skavari, R.V., 1976. Maintenance of genetic homogeneity in systems with multiple genomes. *Genet. res.* 27, 249–265.
- Calderón, I., Garrabou, J., Aurelle, D., 2006. Evaluation of the utility of COI and ITS markers as tools for population genetic studies of temperate gorgonians. *J. Exp. Mar. Biol. Ecol.* 336, 184–197.
- Chase, M.W., Salamin, N., Wilkinson, M., Dunwell, J.M., Kesanakurthi, R.P., Haidar, N., Savolainen, V., 2005. Land plants and DNA barcodes: short-term and long-term goals. *Phil. Trans. R. Soc. B* 360, 1889–1895.
- Chen, C., Chang, C., Wei, N., Chen, C., Lein, Y., Lin, H., Dai, C., Wallace, C., 2004. Secondary structure and phylogenetic utility of the ribosomal internal transcribed spacer 2 (ITS2) in scleractinian corals. *Zool. Stud.* 43, 759–771.
- Coleman, A.W., Vacquier, V.D., 2002. Exploring the phylogenetic utility of ITS sequences for animals: a test case for abalone (*Haliotis*). *J. Mol. Evol.* 54, 246–257.
- Colgan, M., 1984. The Cretaceous Coral *Heliopora* (Octocorallia, Coenothecalia)—a Common Indo-Pacific Reef Builder. In: Eldredge, N., Stanley, S. (Eds.), *Living Fossils*. Springer, New York, pp. 266–271.
- Dolan, E., Tyler, P.A., Yesson, C., Rogers, A.D., 2013. Phylogeny and systematics of deep-sea sea pens (Anthozoa: Octocorallia: Pennatulacea). *Mol. Phylogenet. Evol.* 69, 610–618.
- Dorado, D., Sánchez, J.A., 2009. Internal transcribed spacer (ITS2) variation in the gorgonian coral pseudopterogorgiabiopinnata in Belize and Panama. *Smithson. Contrib. Mar. Sci.* 38, 173–179.
- Dover, G.A., 1982. Molecular drive, a cohesive model of species evolution. *Nature* 299, 111.
- Escobar, D., Zea, S., Sánchez, J.A., 2012. Phylogenetic relationships among the Caribbean members of the *Cliona viridis* complex (Porifera, Demospongiae, Hadromerida) using nuclear and mitochondrial DNA sequences. *Mol. Phylogenet. Evol.* 64, 271–284.
- Fabricius, K., Alderslade, P., Science, A.I.O.M., 2001. Soft corals and sea fans: a comprehensive guide to the tropical shallow water genera of the central-west Pacific the Indian Ocean and the Red Sea. *Austr. Inst. Mar. Sci.*
- France, S., Hoover, L., 2002. DNA sequences of the mitochondrial COI gene have low levels of divergence among deep-sea octocorals (Cnidaria: Anthozoa). *Hydrobiologia* 471, 149–155.
- France, S., Rosel, P., Agenboard, J., Mullineaux, L., Kocher, T., 1996. DNA sequence variation of mitochondrial large-subunit rRNA provides support for a two subclass organization of the Anthozoa (Cnidaria). *Mar. Mol. Biol. Biotechnol.* 5, 15–28.
- Fukami, H., Budd, A., Paulay, G., Sole-Cava, A., Chen, C., Iwao, K., Knowlton, N., 2004. Conventional taxonomy obscures deep divergence between Pacific and Atlantic corals. *Nature* 427, 832–832.
- Funk, D., Omland, K., 2003. SPECIES-LEVEL PARAPHYLY AND POLYPHYLY: Frequency, Causes, and Consequences, with Insights from Animal Mitochondrial DNA. *Annu. Rev. Ecol. Syst.* 34, 397–423.
- Grajales, A., Aguilar, C., Sánchez, J., 2007. Phylogenetic reconstruction using secondary structures of internal transcribed spacer 2 (ITS2, rDNA): finding the molecular and morphological gap in Caribbean gorgonian corals. *BMC Evol. Biol.* 7, 90.
- Hebert, P.D.N., Cywinska, A., Ball, S.L., deWaard, J.R., 2003. Biological identifications through DNA barcodes. *Proc. R. Soc. B: Biol. Sci.* 270, 313–321.
- Hellberg, M., 2006. No variation and low synonymous substitution rates in coral mtDNA despite high nuclear variation. *BMC Evol. Biol.* 6, 24.
- Herrera, S., Baco, A., Sánchez, J., 2010. Molecular systematics of the bubblegum coral genera (Paragorgiidae, Octocorallia) and description of a new deep-sea species. *Mol. Phylogenet. Evol.* 55, 123–135.
- Hollingsworth, P.M., Graham, S.W., Little, D.P., 2011. Choosing and Using a Plant DNA Barcode. *PLoS ONE* 6, e19254.
- Huang, D., Meier, R., Todd, P., Chou, L., 2008. Slow mitochondrial COI sequence evolution at the base of the metazoan tree and its implications for DNA barcoding. *J. Mol. Evol.* 66, 167–174.
- Jakobsson, M., Rosenberg, N.A., 2007. CLUMPP: a cluster matching and permutation program for dealing with label switching and multimodality in analysis of population structure. *Bioinformatics* 23, 1801–1806.
- Kim, E., Lasker, H., Coffroth, M., Kim, K., 2004. Morphological and genetic variation across reef habitats in a broadcast-spawning octocoral. In: Fautin, D., Westfall, J., Cartwright, P., Daly, M., Wyttenbach, C.R. (Eds.), *Coelenterate Biology 2003*. Springer, Netherlands, pp. 423–432.
- Kingman, J.F.C., 1982. The coalescent. *Stochastic Process. Appl.* 13, 235–248.
- Lajeunesse, T.C., Pinzón, J.H., 2007. Screening intragenomic rDNA for dominant variants can provide a consistent retrieval of evolutionarily persistent ITS (rDNA) sequences. *Mol. Phylogenet. Evol.* 45, 417–422.
- Librado, P., Rozas, J., 2009. DnaSP v5: A software for comprehensive analysis of DNA polymorphism data. *Bioinformatics* 25, 1451–1452.
- Lorenz, J.G., Jackson, W.E., Beck, J.C., Hanner, R., 2005. The problems and promise of DNA barcodes for species diagnosis of primate biomaterials. *Phil. Trans. R. Soc. B* 360, 1869–1877.
- Luikart, G., Allendorf, F., Cornuet, J.-M., Sherwin, W., 1998. Distortion of allele frequency distributions provides a test for recent population bottlenecks. *J. Hered.* 89, 238–247.
- Marquez, L.M., Miller, D.J., MacKenzie, J.B., Van Oppen, M.J., 2003. Pseudogenes contribute to the extreme diversity of nuclear ribosomal DNA in the hard coral *Acropora*. *Mol. Biol. Evol.* 20, 1077–1086.
- McFadden, C., Benayahu, Y., Pante, E., Thoma, J., Nevarez, P., France, S., 2011. Limitations of mitochondrial gene barcoding in Octocorallia. *Mol. Ecol. Resour.* 11, 19–31.
- McFadden, C., France, S., Sánchez, J., Alderslade, P., 2006. A molecular phylogenetic analysis of the Octocorallia (Cnidaria: Anthozoa) based on mitochondrial protein-coding sequences. *Mol. Phylog. Evol.* 41, 513–527.
- McFadden, C.S., Sánchez, J.A., France, S.C., 2010. Molecular Phylogenetic Insights into the Evolution of Octocorallia: A Review. *Integr. Comp. Biol.* 50.
- Mi-Hyun, P., Chung-Ja, S., Jina, B., Gi-Sik, M., 2007. Identification of genes suitable for DNA barcoding of morphologically indistinguishable Korean Halichondriidae sponges. *Mol. Cells* 23, 220–227.
- Moritz, C., Cicero, C., 2004. DNA barcoding: promise and pitfalls. *PLoS Biol.* 2, e354.
- Muller, T., Philippi, N., Dandekar, T., Schultz, J., Wolf, M., 2007. Distinguishing species. *RNA (New York, N.Y.)* 13, 1469–1472.
- Nei, M., 1987. *Molecular Evolutionary Genetics*. Columbia University Press, p. 512.
- Peakall, R., Smouse, P.E., 2005. GenAlEx 6: Genetic Analysis in Excel. In: *Population genetic software for teaching and research*, sixth ed. Australian National University, Canberra, Australia.
- Piry, S., Luikart, G., Cornuet, J.M., 1999. BOTTLENECK: a computer program for detecting recent reductions in the effective population size using allele frequency data. *J. Hered.* 90, 502–503.
- Prada, C., Schizas, N., Yoshioka, P., 2008. Phenotypic plasticity or speciation? A case from a clonal marine organism. *BMC Evol. Biol.* 8, 47.

- Pritchard, J.K., Stephens, M., Donnelly, P., 2000. Inference of population structure using multilocus genotype data. *Genetics* 155, 945–959.
- Romano, S., Palumbi, S., 1996. Evolution of scleractinian corals inferred from molecular systematics. *Science* 271, 640–642.
- Saito, Y., Ueno, M., Kiatano, Y.F., Yasuda, N., 2015. Potential of different reproductive timing between sympatric *Heliopora coerulea* lineages southeast of Iriomote Island, Japan. *Bul. Mar. Sci.* 91. <http://dx.doi.org/10.5343/bms.2015.1024>.
- Sánchez, J.A., Dorado, D., 2008. Intragenomic ITS2 variation in Caribbean seafans. *Proc. 11th Int. Coral Reef Sympo.* 26, 1383–1387.
- Shearer, T., van Oppen, M., Romano, S., Worheide, G., 2002. Slow mitochondrial DNA sequence evolution in the Anthozoa (Cnidaria). *Mol. Ecol.* 11, 2475–2487.
- Tajima, F., 1983. Evolutionship of DNA sequences in finite populations. *Genetics* 105, 437–460.
- Tamura, K., 1992. Estimation of the number of nucleotide substitutions when there are strong transition–transversion and G+C-content biases. *Mol. Biol. Evol.* 9, 678–687.
- Tamura, K., Nei, M., 1993. Estimation of the number of nucleotide substitutions in the control region of mitochondrial DNA in humans and chimpanzees. *Mol. Biol. Evol.* 10, 512–526.
- Tamura, K., Stecher, G., Peterson, D., Filipski, A., Kumar, S., 2013. MEGA6: Molecular evolutionary genetics analysis version 6.0. *Mol. Biol. Evol.* 30, 2725–2729.
- Thornhill, D.J., Lajeunesse, T.C., Santos, S.R., 2007. Measuring rDNA diversity in eukaryotic microbial systems: how intragenomic variation, pseudogenes, and PCR artifacts confound biodiversity estimates. *Mol. Ecol.* 16, 5326–5340.
- Torres-Suarez, O.L., 2014. *Gorgonia mariae* and *Antillogorgia bipinnata* populations inferred from compensatory base change analysis of the internal transcribed spacer 2. *Mol. Phylogenet. Evol.* 79, 240–248.
- van Oppen, M., Willis, B., Miller, D., 1999. Atypically low rate of cytochrome b evolution in the scleractinian coral genus *Acropora*. *Proc. R. Soc. Lond. B* 266, 179–183.
- Waugh, J., 2007. DNA barcoding in animal species: progress, potential and pitfalls. *BioEssays* 29, 188–197.
- Wei, N., Wallace, C., Dai, C., Pillay, R., Chen, C., 2006. Analyses of the ribosomal internal transcribed spacers (ITS) and the 5.8S gene indicate that extremely high rDNA heterogeneity is a unique feature in the scleractinian cora genus *Acropora* (Scleractinia:Acroporidae). *Zool. Stud.* 45, 404–418.
- Weider, L., Elser, J., Crease, T., Mateos, M., Cotner, J., Markow, T., 2005. THE Functional Significance of ribosomal (r)DNA variation: impacts on the evolution of ecology of organisms. *Annu. Rev. Ecol. Evol. Syst.* 36, 219–242.
- Wörheide, G., 2006. Low variation in partial cytochrome oxidase subunit I (COI) mitochondrial sequences in the coralline demosponge *Astrosclera willeyana* across the Indo-Pacific. *Mar. Biol.* 148, 907–912.
- Yang, H.Q., Dong, Y.R., Gu, Z.J., Liang, N., Yang, J.B., 2012. A Preliminary Assessment of matK, rbcL and trnH-psbA as DNA Barcodes for *Calamus* (Arecaceae) species in China with a Note on ITS. *Ann. Bot. Fenn.* 49, 319–330.
- Yasuda, N., Nagai, S., Lian, C., Hamaguchi, M., Hayashibara, T., Nadaoka, K., 2008. Identification and characterization of microsatellite loci in the blue coral *Heliopora coerulea* (Alcyonaria: Coenothecalia). *Conserv. Genet.* 9, 1011–1013.
- Yasuda, N., Takino, T., Kimura, M., Lian, C.L., Nagai, S., Nadaoka, K., 2010. Genetic structuring across the reef crest in the threatened blue coral *Heliopora coerulea* (Helioporidae, Octacorallia) in Shiraho Reef, southwest Japan. In: Urbano, V.K. (Ed.), *Advances in Genetics Research*. Nova Science Publishers, New York, pp. 315–324.
- Yasuda, N., Taquet, C., Nagai, S., Fortes, M., Fan, T.Y., Phongsuwan, N., Nadaoka, K., 2004. Genetic structure and cryptic speciation in the threatened reef-building coral *Heliopora coerulea* along Kuroshio Current. *B. Mar. Sci.* 90, 233–255.
- Zuker, M., 2003. Mfold web server for nucleic acid folding and hybridization prediction. *Nucleic. Acids. Res.* 31, 3406–3415.